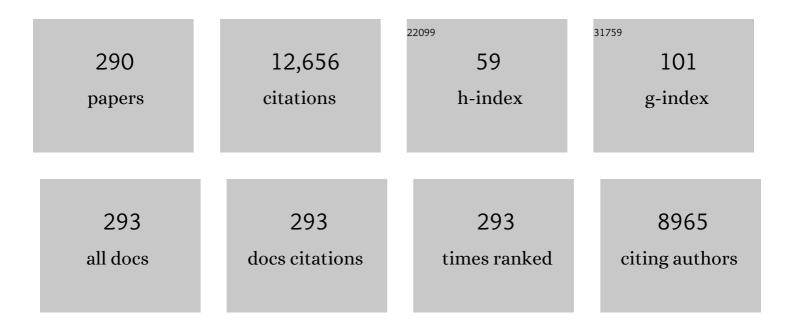
Raffaele Giordano

List of Publications by Year in descending order

Source: https://exaly.com/author-pdf/5027375/publications.pdf Version: 2024-02-01



#	Article	IF	CITATIONS
1	Congenital heart disease in the era of COVID-19 pandemic. General Thoracic and Cardiovascular Surgery, 2021, 69, 172-174.	0.4	14
2	Intracardiac flow visualization using highâ€frame rate blood speckle tracking echocardiography: Illustrations from infants with congenital heart disease. Echocardiography, 2021, 38, 707-715.	0.3	9
3	A statistical comparison of reproducibility in current pediatric two-dimensional echocardiographic nomograms. Pediatric Research, 2021, 89, 579-590.	1.1	6
4	Pediatric ranges of normality for 2D speckleâ€tracking echocardiography atrial strain: differences between p†and râ€gating and among new (Atrial Designed) and conventional (Ventricular Specific) software's. Echocardiography, 2021, 38, 2025-2031.	0.3	4
5	Frame-Level Intermodular Configuration Scrubbing of On-Detector FPGAs for the ARICH at Belle II. IEEE Transactions on Nuclear Science, 2021, 68, 2810-2817.	1.2	4
6	Echocardiographic examination of mitral valve abnormalities in the paediatric population: current practices. Cardiology in the Young, 2020, 30, 1-11.	0.4	14
7	A Radiation-Tolerant, Multigigabit Serial Link Based on FPGAs. IEEE Transactions on Nuclear Science, 2020, 67, 1852-1860.	1.2	2
8	Pediatric nomograms for left ventricle biplane 2D volumes in healthy Caucasian children. Echocardiography, 2020, 37, 971-975.	0.3	6
9	On-the-Fly Self-Reconfiguring FPGAs for Single Event Upset Monitoring at Belle II. , 2020, , .		Ο
10	Double Orifice Mitral Valve in Tricuspid Atresia: A Rare Association. Pediatric Cardiology, 2019, 40, 1761-1762.	0.6	0
11	Three-Dimensional Echocardiography Derived Nomograms for Left Ventricular Volumes in Healthy Caucasian Italian Children. Journal of the American Society of Echocardiography, 2019, 32, 794-797.e1.	1.2	8
12	Nomograms of pulsed Doppler velocities, times, and velocity time integrals for semilunar valves and great arteries in healthy Caucasian children. International Journal of Cardiology, 2019, 285, 133-139.	0.8	1
13	The FAZIA setup: A review on the electronics and the mechanical mounting. Nuclear Instruments and Methods in Physics Research, Section A: Accelerators, Spectrometers, Detectors and Associated Equipment, 2019, 930, 27-36.	0.7	28
14	Custom Scrubbing for Robust Configuration Hardening in Xilinx FPGAs. Instruments, 2019, 3, 56.	0.8	7
15	Self-contained configuration scrubbing in Xilinx FPGAs for on-detector applications. Nuclear Instruments and Methods in Physics Research, Section A: Accelerators, Spectrometers, Detectors and Associated Equipment, 2019, 936, 363-365.	0.7	0
16	First measurements of beam backgrounds at SuperKEKB. Nuclear Instruments and Methods in Physics Research, Section A: Accelerators, Spectrometers, Detectors and Associated Equipment, 2019, 914, 69-144.	0.7	38
17	Left and Right Atrial Strain in Healthy Caucasian Children by Two-Dimensional Speckle-Tracking Echocardiography. Journal of the American Society of Echocardiography, 2019, 32, 165-168.e3.	1.2	18
18	Nomograms for Cardiovascular Magnetic Resonance Measurements in the Pediatric Age Group: To Define the Normal and the Expected Abnormal Values in Corrected/Palliated Congenital Heart Disease: A Systematic Review. Journal of Magnetic Resonance Imaging, 2019, 49, 1222-1235.	1.9	6

#	Article	IF	CITATIONS
19	A New Interface Board for the Level-1 Muon Barrel Trigger Upgrade of the ATLAS Experiment. IEEE Transactions on Nuclear Science, 2019, 66, 1028-1035.	1.2	0
20	Right thoracotomy for aortic valve replacement in the adolescents with bicuspid aortic valve. Congenital Heart Disease, 2019, 14, 162-166.	0.0	1
21	Lung ultrasound reclassification of chest Xâ€ray data after pediatric cardiac surgery. Paediatric Anaesthesia, 2018, 28, 421-427.	0.6	31
22	Use of linear and convex ultrasound transducers for evaluation of retrosternal area in patients after cardiac surgery. Echocardiography, 2018, 35, 100-103.	0.3	4
23	Normative Data for Left and Right Ventricular Systolic Strain in Healthy Caucasian ItalianÂChildren by Two-Dimensional Speckle-Tracking Echocardiography. Journal of the American Society of Echocardiography, 2018, 31, 712-720.e6.	1.2	39
24	Strengths, Limitations, and Geographical Discrepancies in the Eligibility Criteria for Sport Participation in Young Patients With Congenital Heart Disease. Clinical Journal of Sport Medicine, 2018, 28, 540-560.	0.9	2
25	Nomograms for echocardiographic right ventricular sub-costal view dimensions in healthy Caucasian children: A new approach to measure the right ventricle. Journal of Cardiology, 2018, 71, 181-186.	0.8	2
26	Incidence and natural history of neonatal isolated ventricular septal defects: Do we know everything? A 6-year single-center Italian experience follow-up. Congenital Heart Disease, 2018, 13, 105-112.	0.0	25
27	Echocardiographic nomograms for upper abdominal aorta Doppler systolic wave values and systo-diastolic diameters variations in children. Journal of Cardiology, 2018, 71, 394-400.	0.8	3
28	Impact of 3D printing on the surgical management of tracheal stenosis associated to pulmonary sling: a case report. Journal of Thoracic Disease, 2018, 10, E130-E133.	0.6	11
29	Comparison of the different cardioplegic strategies in cardiac valves surgery: who wins the "arm-wrestling�. Journal of Thoracic Disease, 2018, 10, 714-717.	0.6	15
30	Female gender and left ventricular dysfunction in myocardial surgical revascularization: the strange couple. Journal of Thoracic Disease, 2018, 10, S2160-S2164.	0.6	0
31	Endovascular treatment for chronic type B aortic dissection: current opinions. Journal of Thoracic Disease, 2018, 10, S978-S982.	0.6	6
32	A Self-Repairing and Adaptive FPGA-based High-speed Serial Link. , 2018, , .		1
33	Beam and Field Testing of Configuration Self-repair in Xilinx FPGAs. , 2018, , .		0
34	Limitations of Current Fetal Echocardiography Nomograms for 2D Measures: A Critical Overview and Analysis for Future Research. Journal of the American Society of Echocardiography, 2018, 31, 1368-1372.e10.	1.2	2
35	Configuration Self-Repair in Xilinx FPGAs. IEEE Transactions on Nuclear Science, 2018, 65, 2691-2698.	1.2	9
36	The Fate of the Tricuspid Valve After the Transatrial Closure of the Ventricular Septal Defect. Annals of Thoracic Surgery, 2018, 106, 1229-1233.	0.7	7

#	Article	IF	CITATIONS
37	Study of Radiation-Induced Soft-Errors in FPGAs for Applications at High-Luminosity \$\$e^+e^-\$\$ Colliders. Springer Proceedings in Physics, 2018, , 386-390.	0.1	0
38	A Service-Oriented Platform for Embedded Monitoring Systems in Belle II Experiment. Springer Proceedings in Physics, 2018, , 54-57.	0.1	0
39	Nomograms for two-dimensional echocardiography derived valvular and arterial dimensions in Caucasian children. Journal of Cardiology, 2017, 69, 208-215.	0.8	35
40	A JESD204B-Compliant Architecture for Remote and Deterministic-Latency Operation. IEEE Transactions on Nuclear Science, 2017, 64, 1225-1231.	1.2	6
41	Arterial Switch Operation and Plasma Biomarkers: Analysis and Correlation with Early Postoperative Outcomes. Pediatric Cardiology, 2017, 38, 1071-1076.	0.6	8
42	uSOP: A Microprocessor-Based Service-Oriented Platform for Control and Monitoring. IEEE Transactions on Nuclear Science, 2017, 64, 1185-1190.	1.2	5
43	Diagnostic accuracy and prognostic valued of plasmatic Cystatin-C in children undergoing pediatric cardiac surgery. Clinica Chimica Acta, 2017, 471, 113-118.	0.5	6
44	Echocardiographic assessment of pediatric semilunar valve disease. Echocardiography, 2017, 34, 1360-1370.	0.3	10
45	Impact of different values of prosthesis–patient mismatch on outcome in male patients with aortic valve replacement. Journal of Cardiovascular Medicine, 2017, 18, 366-373.	0.6	8
46	Redundant-Configuration Scrubbing of SRAM-Based FPGAs. IEEE Transactions on Nuclear Science, 2017, 64, 2497-2504.	1.2	27
47	Monitoring complex detectors: the uSOP approach in the Belle II experiment. Journal of Instrumentation, 2017, 12, C08003-C08003.	0.5	0
48	A Time-to-Digital Converter Based on a Digitally Controlled Oscillator. IEEE Transactions on Nuclear Science, 2017, , 1-1.	1.2	3
49	The upgrade of the Belle II forward calorimeter. Nuclear Instruments and Methods in Physics Research, Section A: Accelerators, Spectrometers, Detectors and Associated Equipment, 2017, 845, 524-527.	0.7	0
50	First Experience With Levosimendan Therapy After Correction of Congenital Heart Disease. Journal of Cardiothoracic and Vascular Anesthesia, 2017, 31, e19-e21.	0.6	3
51	The Reorganize and Multiplex (RMU) front-end trigger optical bridge for the JUNO experiment. , 2017, , .		0
52	Highâ€Speed Deterministic‣atency Serial IO. , 2017, , .		0
53	The BELLE Electromagnetic Calorimeter and its Upgrade to Bellell. Journal of Instrumentation, 2017, 12, C07032-C07032.	0.5	0
54	Monitoring single event upsets in SRAM-based FPGAs at the SuperKEKB interaction point. Journal of Instrumentation, 2017, 12, C07039-C07039.	0.5	2

#	Article	IF	CITATIONS
55	Adult echocardiographic nomograms: overview, critical review and creation of a software for automatic, fast and easy calculation of normal values. Journal of Thoracic Disease, 2017, 9, 5404-5422.	0.6	4
56	Surgical strategy for tetralogy of Fallot with abnormal coronary arteries. Journal of Thoracic Disease, 2017, 9, 3447-3449.	0.6	8
57	To do or not to do? The management dilemma of congenital tracheal stenosis in the setting of the ring-sling complex. Journal of Thoracic Disease, 2017, 9, 4896-4898.	0.6	13
58	Lung ultrasound: a new basic, easy, multifunction imaging diagnostic tool in children undergoing pediatric cardiac surgery. Journal of Thoracic Disease, 2017, 9, 1396-1399.	0.6	5
59	Strengths and Limitations of Current Adult Nomograms for the Aorta Obtained by Noninvasive Cardiovascular Imaging. Echocardiography, 2016, 33, 1046-1068.	0.3	6
60	A JESD204B-compliant architecture for remote and deterministic-latency operation. , 2016, , .		1
61	A pure CsI calorimeter for the Belle II experiment at SuperKEKB. Nuclear Instruments and Methods in Physics Research, Section A: Accelerators, Spectrometers, Detectors and Associated Equipment, 2016, 824, 704-709.	0.7	2
62	Custodiol Solution and Cold Blood Cardioplegia in Arterial Switch Operation: Retrospective Analysis in a Single Center. Thoracic and Cardiovascular Surgeon, 2016, 64, 053-058.	0.4	14
63	uSOP: A microprocessor-based service-oriented platform for control and monitoring. , 2016, , .		1
64	Major Aortopulmonary Collaterals in Transposition of the Great Arteries: A Cause for Preoperative and Postoperative Hemodynamic Imbalance. Annals of Thoracic Surgery, 2016, 102, e33-e35.	0.7	7
65	A time-to-digital converter based on a digitally controlled oscillator. , 2016, , .		3
66	A fully-digital and fully synthetizable TDC for high energy physics experiments. , 2016, , .		2
67	Soft-errors in FPGAs at the SuperKEKB interaction point. , 2016, , .		0
68	Measurement of the centrality dependence of the charged-particle pseudorapidity distribution in proton–lead collisions at \$\$sqrt{s_{_ext {NN}} = 5.02\$\$ s NN = 5.02 ÂTeV with the ATLAS detector. European Physical Journal C, 2016, 76, 199.	1.4	60
69	Lung ultrasound in adult and paediatric cardiac surgery: is it time for routine use?. Interactive Cardiovascular and Thoracic Surgery, 2016, 22, 208-215.	0.5	21
70	Nomograms for mitral inflow Doppler and tissue Doppler velocities in Caucasian children. Journal of Cardiology, 2016, 68, 288-299.	0.8	28
71	Congenitally palliated scimitar syndrome. Cardiology in the Young, 2015, 25, 1218-1220.	0.4	3
72	Measurement of the forward-backward asymmetry of electron and muon pair-production in pp collisions at s = 7 \$\$ sqrt{s}=7 \$\$ TeV with the ATLAS detector. Journal of High Energy Physics, 2015, 2015, 1.	1.6	28

#	Article	IF	CITATIONS
73	Differential top-antitop cross-section measurements as a function of observables constructed from final-state particles using pp collisions at s = 7 \$\$ sqrt{s}=7 \$\$ TeV in the ATLAS detector. Journal of High Energy Physics, 2015, 2015, 1.	1.6	40
74	Search for new phenomena in events with three or more charged leptons in pp collisions at s = 8 \$\$ sqrt{s}=8 \$\$ TeV with the ATLAS detector. Journal of High Energy Physics, 2015, 2015, 1.	1.6	20
75	Supra-Annular Mitral Valve Implantation in Very Small Children. Journal of Cardiac Surgery, 2015, 30, 185-189.	0.3	9
76	First experience with sildenafil after Fontan operation. Journal of Cardiovascular Medicine, 2015, 16, 552-555.	0.6	20
77	Search for squarks and gluinos in events with isolated leptons, jets and missing transverse momentum at s = 8 \$\$ sqrt{s}=8 \$\$ TeV with the ATLAS detector. Journal of High Energy Physics, 2015, 2015, 1.	1.6	42
78	Evidence for the Higgs-boson Yukawa coupling to tau leptons with the ATLAS detector. Journal of High Energy Physics, 2015, 2015, 1.	1.6	116
79	Measurement of the charge asymmetry in dileptonic decays of top quark pairs in pp collisions at s = 7 \$\$ sqrt{s}=7 \$\$ TeV using the ATLAS detector. Journal of High Energy Physics, 2015, 2015, 1.	1.6	17
80	Search for \$\$W' ightarrow tb ightarrow qqbb\$\$ W ′ → t b → q q b b decays in \$\$pp\$\$ p p collisions at \$\$sqrt{s}\$\$ s Â=Ă8ÂTeV with the ATLAS detector. European Physical Journal C, 2015, 75, 165.	1.4	35
81	Measurement of the top-quark mass in the fully hadronic decay channel from ATLAS data at \$\$sqrt{s}=7mathrm{,TeV}\$\$ s = 7 TeV. European Physical Journal C, 2015, 75, 158.	1.4	17
82	Layout and Radiation Tolerance Issues in High-Speed Links. IEEE Transactions on Nuclear Science, 2015, 62, 3177-3185.	1.2	3
83	High-Resolution Synthesizable Digitally-Controlled Delay Lines. IEEE Transactions on Nuclear Science, 2015, 62, 3163-3171.	1.2	23
84	Measurement of the production and lepton charge asymmetry of \$\$W\$\$ W bosons in Pb+Pb collisions at \$\$mathbf {sqrt{mathbf {s}_{mathrm {mathbf {NN}}}=2.76;TeV}\$\$ s NN = 2.76 TeV with the ATLAS detector. European Physical Journal C, 2015, 75, 23.	1.4	41
85	A Frequency Agile, Self-Adaptive Serial Link on Xilinx FPGAs. IEEE Transactions on Nuclear Science, 2015, 62, 955-962.	1.2	2
86	Chest Ultrasound: A New, Easy, and Radiation-Free Tool to Detect Retrosternal Clot After Pediatric Cardiac Surgery. Journal of Cardiothoracic and Vascular Anesthesia, 2015, 29, e59-e60.	0.6	12
87	Prognostic role of BNP in children undergoing surgery for congenital heart disease: analysis of prediction models incorporating standard risk factors. Clinical Chemistry and Laboratory Medicine, 2015, 53, 1839-46.	1.4	28
88	Jet energy measurement and its systematic uncertainty in proton–proton collisions at \$\$sqrt{s}=7\$\$ s = 7 ÅTeV with the ATLAS detector. European Physical Journal C, 2015, 75, 17.	1.4	268
89	Search for invisible particles produced in association with single-top-quarks in proton–proton collisions at \$\$sqrt{s}=mathrm {8~TeV}\$\$ s = 8 TeV with the ATLAS detector. European Physical Journal C, 2015, 75, 79.	1.4	30
90	Search for resonant diboson production in the \$\$mathrm {ell ell }qar{q}\$\$ â"" â"" q q Â⁻ final state in \$\$pp\$\$ p p collisions at \$\$sqrt{s} = 8\$\$ s = 8 ÂTeV with the ATLAS detector. European Physical Journal C, 2015, 75, 69.	1.4	74

#	Article	IF	CITATIONS
91	Measurements of the \$\$W\$\$ W production cross sections in association with jets with the ATLAS detector. European Physical Journal C, 2015, 75, 82.	1.4	92
92	Search for dark matter in events with heavy quarks and missing transverse momentum in \$\$pp\$\$ p p collisions with the ATLAS detector. European Physical Journal C, 2015, 75, 92.	1.4	77
93	Measurement of the t t Â ⁻ \$\$ toverline{t} \$\$ production cross-section as a function of jet multiplicity and jet transverse momentum in 7 TeV proton-proton collisions with the ATLAS detector. Journal of High Energy Physics, 2015, 2015, 1.	1.6	30
94	Measurement of the W W + W Z cross section and limits on anomalous triple gauge couplings using final states with one lepton, missing transverse momentum, and two jets with the ATLAS detector at s = 7 \$\$ sqrt{s}=7 \$\$ TeV. Journal of High Energy Physics, 2015, 2015, 1.	1.6	27
95	Searches for heavy long-lived charged particles with the ATLAS detector in proton-proton collisions at s = 8 \$\$ sqrt{s}=8 \$\$ TeV. Journal of High Energy Physics, 2015, 2015, 1.	1.6	33
96	Search for the b b \hat{A}^- \$\$ boverline{b} \$\$ decay of the Standard Model Higgs boson in associated (W/Z)H production with the ATLAS detector. Journal of High Energy Physics, 2015, 2015, 1.	1.6	89
97	Measurement of the inclusive jet cross-section in proton-proton collisions at s = 7 \$\$ sqrt{s}=7 \$\$ TeV using 4.5 fbâ^'1 of data with the ATLAS detector. Journal of High Energy Physics, 2015, 2015, 1.	1.6	35
98	Search for anomalous production of prompt same-sign lepton pairs and pair-produced doubly charged Higgs bosons with s = 8 \$\$ sqrt{s}=8 \$\$ TeV pp collisions using the ATLAS detector. Journal of High Energy Physics, 2015, 2015, 1.	1.6	60
99	Search for charged Higgs bosons decaying via H ± → Ï,, ± ν in fully hadronic final states using pp collision data at s \$\$ sqrt{s} \$\$ = 8 TeV with the ATLAS detector. Journal of High Energy Physics, 2015, 2015, 1.	1.6	69
100	Seahorse left atrial appendage diverticula mimicking a coronary fistula. Cardiology in the Young, 2015, 25, 550-551.	0.4	0
101	Performance of the ATLAS muon trigger in pp collisions at \$\$sqrt{s}=8\$\$ s = 8 TeV. European Physical Journal C, 2015, 75, 120.	1.4	62
102	Strengths and limitations of current pediatric blood pressure nomograms: a global overview with a special emphasis on regional differences in neonates and infants. Hypertension Research, 2015, 38, 577-587.	1.5	18
103	Measurement of three-jet production cross-sections in \$\$pp\$\$ p p collisions at 7Â \$\$mathrm { Te,V}\$\$ Te V centre-of-mass energy using the ATLAS detector. European Physical Journal C, 2015, 75, 228.	1.4	23
104	Identification and energy calibration of hadronically decaying tau leptons with the ATLAS experiment in pp collisions at \$\$sqrt{s}=8\$\$ s = 8 \$\$,hbox {TeV}\$\$ TeV. European Physical Journal C, 2015, 75, 303.	1.4	70
105	Two-particle Bose–Einstein correlations in pp collisions at \$\$mathbf {sqrt{s} =}\$\$ s = 0.9 and 7 TeV measured with the ATLAS detector. European Physical Journal C, 2015, 75, 466.	1.4	42
106	Review and status report of pediatric left ventricular systolic strain and strain rate nomograms. Heart Failure Reviews, 2015, 20, 601-612.	1.7	25
107	Search for neutral Higgs bosons of the minimal supersymmetric standard model in pp collisions at s = 8 \$\$ sqrt{s}=8 \$\$ TeV with the ATLAS detector. Journal of High Energy Physics, 2014, 2014, 1.	1.6	82
108	Measurement of the muon reconstruction performance of the ATLAS detector using 2011 and 2012 LHC proton–proton collision data. European Physical Journal C, 2014, 74, 3130.	1.4	213

#	Article	IF	CITATIONS
109	Measurements of jet vetoes and azimuthal decorrelations in dijet events produced in \$\$pp\$\$ p p collisions at \$\$sqrt{s}=7,mathrm{TeV}\$\$ s = 7 TeV using the ATLAS detector. European Physical Journal C, 2014, 74, 3117.	1.4	40
110	A measurement of the ratio of the production cross sections for \$\$W\$\$ W and \$\$Z\$\$ Z bosons in association with jets with the ATLAS detector. European Physical Journal C, 2014, 74, 3168.	1.4	23
111	Measurements of fiducial and differential cross sections for Higgs boson production in the diphoton decay channel at s = 8 \$\$ sqrt{s}=8 \$\$ TeV with ATLAS. Journal of High Energy Physics, 2014, 2014, 1.	1.6	45
112	Search for supersymmetry in events with large missing transverse momentum, jets, and at least one tau lepton in 20 fbâ''1 of s \$\$ sqrt{s} \$\$ = 8 TeV proton-proton collision data with the ATLAS detector. Journal of High Energy Physics, 2014, 2014, 1.	1.6	12
113	Search for squarks and gluinos with the ATLAS detector in final states with jets and missing transverse momentum using s = 8 \$\$ sqrt{s}=8 \$\$ TeV proton-proton collision data. Journal of High Energy Physics, 2014, 2014, 1.	1.6	128
114	Measurement of the \$\$toverline{t}\$\$ t t Â ⁻ production cross-section using \$\$emu \$\$ e μ events with \$\$b\$\$ b -tagged jets in \$\$pp\$\$ p p collisions at \$\$sqrt{s}=7\$\$ s = 7 and 8ÂTeV with the ATLAS detector. European Physical Journal C, 2014, 74, 3109.	1.4	143
115	High-resolution synthesizable digitally-controlled delay lines. , 2014, , .		0
116	Layout and radiation tolerance issues in high-speed links for TDAQ systems. , 2014, , .		0
117	Performance of a high-frequency synthesizable digitally-controlled oscillator. , 2014, , .		0
118	A frequency agile, self-adaptive serial link on Xilinx FPGAs. , 2014, , .		0
119	Search for top squark pair production in final states with one isolated lepton, jets, and missing transverse momentum in s \$\$ sqrt{s} \$\$ = 8 TeV pp collisions with the ATLAS detector. Journal of High Energy Physics, 2014, 2014, 1.	1.6	66
120	Muon reconstruction efficiency and momentum resolution of the ATLAS experiment in proton–proton collisions at \$\$sqrt{s}=7\$\$ s = 7 ÂTeV in 2010. European Physical Journal C, 2014, 74, 3034.	1.4	58
121	Electron and photon energy calibration with the ATLAS detector using LHC Run 1 data. European Physical Journal C, 2014, 74, 1.	1.4	172
122	Search for contact interactions and large extra dimensions in the dilepton channel using proton–proton collisions at \$\$sqrt{s}~=\$\$ s = Â8ÂTeV with the ATLAS detector. European Physical Journal C, 2014, 74, 3134.	1.4	48
123	Measurement of flow harmonics with multi-particle cumulants in Pb+Pb collisions at \$\$sqrt{s_{mathrm {NN}}=2.76\$\$ s NN = 2.76 ÂTeV with the ATLAS detector. European Physical Journal C, 2014, 74, 3157.	1.4	68
124	Measurement of distributions sensitive to the underlying event in inclusive Z-boson production in \$\$pp\$\$ p p collisions at \$\$sqrt{s}=7\$\$ s = 7 TeV with the ATLAS detector. European Physical Journal C, 2014, 74, 3195.	1.4	46
125	Search for direct pair production of the top squark in all-hadronic final states in proton-proton collisions at s \$\$ sqrt{s} \$\$ = 8 TeV with the ATLAS detector. Journal of High Energy Physics, 2014, 2014, 1.	1.6	41
126	Measurement of the Z/Î ³ * boson transverse momentum distribution in pp collisions at s = 7 sqrt{s}=7 \$\$ TeV with the ATLAS detector. Journal of High Energy Physics, 2014, 2014, 1.	1.6	131

#	Article	IF	CITATIONS
127	Search for strong production of supersymmetric particles in final states with missing transverse momentum and at least three b-jets at s = 8 \$\$ sqrt{s} = 8 \$\$ TeV proton-proton collisions with the ATLAS detector. Journal of High Energy Physics, 2014, 2014, 1.	1.6	38
128	Measurement of differential production cross-sections for a Z boson in association with b-jets in 7 TeV proton-proton collisions with the ATLAS detector. Journal of High Energy Physics, 2014, 2014, 1.	1.6	45
129	Search for long-lived neutral particles decaying into lepton jets in proton-proton collisions at s = 8 \$\$ sqrt{s}=8 \$\$ TeV with the ATLAS detector. Journal of High Energy Physics, 2014, 2014, 1.	1.6	47
130	Search for pair and single production of new heavy quarks that decay to a Z boson and a third-generation quark in pp collisions at s = 8 \$\$ sqrt{s}=8 \$\$ TeV with the ATLAS detector. Journal of High Energy Physics, 2014, 2014, 1.	1.6	35
131	Measurement of the top quark pair production charge asymmetry in proton-proton collisions at \$ sqrt{s} \$ = 7 TeV using the ATLAS detector. Journal of High Energy Physics, 2014, 2014, 1.	1.6	42
132	The FAZIA project in Europe: R&D phase. European Physical Journal A, 2014, 50, 1.	1.0	63
133	Search for the direct production of charginos, neutralinos and staus in final states with at least two hadronically decaying taus and missing transverse momentum in pp collisions at s = 8 \$\$ sqrt{s}=8 \$\$ TeV with the ATLAS detector. Journal of High Energy Physics, 2014, 2014, 1.	1.6	40
134	The differential production cross section of the \$\$phi \$\$ Ï• (1020) meson in \$\$sqrt{s}\$\$ s = 7ÂTeV \$\$pp\$\$ p p collisions measured with the ATLAS detector. European Physical Journal C, 2014, 74, 2895.	1.4	13
135	Electron reconstruction and identification efficiency measurements with the ATLAS detector using the 2011 LHC proton–proton collision data. European Physical Journal C, 2014, 74, 2941.	1.4	204
136	Measurement of the underlying event in jet events from 7 \$\$ext {TeV}\$\$ TeV proton–proton collisions with the ATLAS detector. European Physical Journal C, 2014, 74, 1.	1.4	23
137	Measurement of the centrality and pseudorapidity dependence of the integrated elliptic flow in lead–lead collisions at \$\$sqrt{s_{mathrm {NN}}}=2.76\$\$ s NN = 2.76 ÂTeVÂwith the ATLAS detector. European Physical Journal C, 2014, 74, 2982.	1.4	22
138	Light-quark and gluon jet discrimination in \$\$pp\$\$ p p collisions at \$\$sqrt{s}=7mathrm { TeV}\$\$ s = 7 TeV with the ATLAS detector. European Physical Journal C, 2014, 74, 3023.	1.4	77
139	Measurement of the electroweak production of dijets in association with a Z-boson and distributions sensitive to vector boson fusion in proton-proton collisions at \$ sqrt{s} \$ = 8 TeV using the ATLAS detector. Journal of High Energy Physics, 2014, 2014, 1.	1.6	22
140	Search for direct production of charginos and neutralinos in events with three leptons and missing transverse momentum in \$ sqrt{s} \$ = 8 TeV pp collisions with the ATLAS detector. Journal of High Energy Physics, 2014, 2014, 1.	1.6	88
141	Measurement of the production cross section of prompt J/i̇̀ mesons in association with a W ± boson in pp collisions at \$ sqrt{s} \$ = 7 TeV with the ATLAS detector. Journal of High Energy Physics, 2014, 2014, 1.	1.6	35
142	Measurement of dijet cross-sections in pp collisions at 7 TeV centre-of-mass energy using the ATLAS detector. Journal of High Energy Physics, 2014, 2014, 1.	1.6	36
143	Measurement of the production of a W boson in association with a charm quark in pp collisions at \$ sqrt{s} \$ = 7 TeV with the ATLAS detector. Journal of High Energy Physics, 2014, 2014, 1.	1.6	59
144	Search for direct production of charginos, neutralinos and sleptons in final states with two leptons and missing transverse momentum in pp collisions at \$ sqrt{s} \$ = 8TeV with the ATLAS detector. Journal of High Energy Physics, 2014, 2014, 1.	1.6	145

#	Article	IF	CITATIONS
145	Search for supersymmetry at \$sqrt{s}\$ = 8 TeV in final states with jets and two same-sign leptons or three leptons with the ATLAS detector. Journal of High Energy Physics, 2014, 2014, 1.	1.6	45
146	Measurement of the low-mass Drell-Yan differential cross section at s \$\$ sqrt{s} \$\$ = 7 TeV using the ATLAS detector. Journal of High Energy Physics, 2014, 2014, 1.	1.6	25
147	Search for direct top-squark pair production in final states with two leptons in pp collisions at \$ sqrt{s} \$ = 8 TeV with the ATLAS detector. Journal of High Energy Physics, 2014, 2014, 1.	1.6	59
148	Measurement of χ c1 and χ c2 production with s \$\$ sqrt{s} \$\$ = 7 TeV pp collisions at ATLAS. Journal of High Energy Physics, 2014, 2014, 1.	1.6	32
149	Search for microscopic black holes and string balls in final states with leptons and jets with the ATLAS detector at s \$\$ sqrt{s} \$\$ = 8 TeV. Journal of High Energy Physics, 2014, 2014, 1.	1.6	10
150	Search for new particles in events with one lepton and missing transverse momentum in pp collisions at s \$\$ sqrt{s} \$\$ = 8 TeV with the ATLAS detector. Journal of High Energy Physics, 2014, 2014, 1.	1.6	45
151	Search for direct top squark pair production in events with a \$\$Z\$\$ Z boson, \$\$b\$\$ b -jets and missing transverse momentum in \$\$sqrt{s}=8\$\$ s = 8 TeV \$\$pp\$\$ p p collisions with the ATLAS detector. European Physical Journal C, 2014, 74, 2883.	1.4	55
152	Impact of preoperative antiplatelet therapy on in-hospital outcomes after coronary artery bypass grafting. European Journal of Cardio-thoracic Surgery, 2014, 46, 335-335.	0.6	2
153	APD readout for Belle II endcap calorimeter upgrade with undoped Cesium Iodide crystals. , 2014, , .		0
154	Measurement of the production cross section of jets in association with a Z boson in pp collisions at \$ sqrt{s}=7 \$ TeV with the ATLAS detector. Journal of High Energy Physics, 2013, 2013, 1.	1.6	73
155	Measurement of the cross-section for W boson production in association with b-jets in pp collisions at \$ sqrt{s}=7 \$ TeV with the ATLAS detector. Journal of High Energy Physics, 2013, 2013, 1.	1.6	53
156	Search for third generation scalar leptoquarks in pp collisions at \$ sqrt{s}=7 \$ TeV with the ATLAS detector. Journal of High Energy Physics, 2013, 2013, 1.	1.6	32
157	Search for dark matter candidates and large extra dimensions in events with a jet and missing transverse momentum with the ATLAS detector. Journal of High Energy Physics, 2013, 2013, 1.	1.6	137
158	Measurement of ZZ production in pp collisions at \$ sqrt{s}=7 \$ TeV and limits on anomalous ZZZ and ZZÎ ³ couplings with the ATLAS detector. Journal of High Energy Physics, 2013, 2013, 1.	1.6	61
159	Search for charged Higgs bosons through the violation of lepton universality in \$ toverline{t} \$ events using pp collision data at \$ sqrt{s}=7 \$ TeV with the ATLAS experiment. Journal of High Energy Physics, 2013, 2013, 1.	1.6	19
160	Search for the neutral Higgs bosons of the minimal supersymmetric standard model in pp collisions at \$ sqrt{s}=7 \$ TeV with the ATLAS detector. Journal of High Energy Physics, 2013, 2013, 1.	1.6	52
161	Measurement of k T splitting scales in W→â,,"ν events at \$sqrt{s} = 7 mathrm{TeV}\$ with the ATLAS detector. European Physical Journal C, 2013, 73, 2432.	1.4	19
162	Search for a light charged Higgs boson in the decay channel \$H^{+} ightarrow car{s}\$ in \$tar{t}\$ events using pp collisions at \$sqrt{s} = 7 mathrm{TeV}\$ with the ATLAS detector. European Physical Journal C, 2013, 73, 2465.	1.4	119

#	Article	IF	CITATIONS
163	Power Consumption Versus Configuration SEUs in Xilinx Virtex-5 FPGAs. IEEE Transactions on Nuclear Science, 2013, 60, 3502-3507.	1.2	4
164	Search for direct third-generation squark pair production in final states with missing transverse momentum and two b-jets in \$ sqrt{s}=8 \$ TeV pp collisions with the ATLAS detector. Journal of High Energy Physics, 2013, 2013, 1.	1.6	102
165	Search for new phenomena in final states with large jet multiplicities and missing transverse momentum at \$ sqrt{s}=8 \$ TeV proton-proton collisions using the ATLAS experiment. Journal of High Energy Physics, 2013, 2013, 1.	1.6	71
166	Measurement of the differential cross-section of B + meson production in pp collisions at \$ sqrt{s}=7 \$ TeV at ATLAS. Journal of High Energy Physics, 2013, 2013, 1.	1.6	31
167	Performance of jet substructure techniques for large-R jets in proton-proton collisions at \$ sqrt{s}=7 \$ TeV using the ATLAS detector. Journal of High Energy Physics, 2013, 2013, 1.	1.6	52
168	Improved luminosity determination in pp collisions at \$sqrt {s} = 7 mathrm{TeV}\$ using the ATLAS detector at the LHC. European Physical Journal C, 2013, 73, 2518.	1.4	362
169	Measurement of the inclusive jet cross-section in pp collisions at \$sqrt{s}=2.76 mbox{TeV}\$ and comparison to the inclusive jet cross-section at \$sqrt{s} =7 mbox{TeV}\$ using the ATLAS detector. European Physical Journal C, 2013, 73, 2509.	1.4	105
170	Multi-channel search for squarks and gluinos in \$sqrt{s}=7mbox{ TeV}\$ pp collisions with the ATLAS detector at the LHC. European Physical Journal C, 2013, 73, 2362.	1.4	34

#	Article	IF	CITATIONS
181	Measurement of the flavour composition of dijet events in pp collisions at \$sqrt{s}=7 mbox{TeV}\$ with the ATLAS detector. European Physical Journal C, 2013, 73, 1.	1.4	15
182	Single hadron response measurement and calorimeter jet energy scale uncertainty with the ATLAS detector at the LHC. European Physical Journal C, 2013, 73, 1.	1.4	45
183	Jet energy resolution in proton-proton collisions at \$sqrt{mathrm{s}}=7mbox{ TeV}\$ recorded in 2010 with the ATLAS detector. European Physical Journal C, 2013, 73, 2306.	1.4	209
184	Measurement of the \$tar{t}\$ production cross section in the tau + jets channel using the ATLAS detector. European Physical Journal C, 2013, 73, 2328.	1.4	45
185	B-type natriuretic peptide as a biochemical marker of left ventricular diastolic function: assessment in asymptomatic patients 1 year after valve replacement for aortic stenosis. Interactive Cardiovascular and Thoracic Surgery, 2013, 17, 371-377.	0.5	13
186	Search forWHproduction with a light Higgs boson decaying to prompt electron-jets in proton–proton collisions at \$sqrt {s}=7\$ TeV with the ATLAS detector. New Journal of Physics, 2013, 15, 043009.	1.2	15
187	Design, implementation and test of the timing trigger and control receiver for the LHC. Journal of Instrumentation, 2013, 8, T02003-T02003.	0.5	4
188	Testing radiation tolerance of optical transceivers for the SuperB experiment. , 2012, , .		0
189	FPGA-based serial links for SuperB: Design Issues Vs. Radiation Tolerance. , 2012, , .		Ο
190	S-LINK on a Chip for Embedded Applications. , 2012, , .		0
191	Protocol-independent, fixed-latency links with FPGA-embedded SerDeses. Journal of Instrumentation, 2012, 7, P05004-P05004.	0.5	20
192	Measurement of the cross section for top-quark pair production in pp collisions at \$sqrt {s} = {7},{ext{TeV}}\$ with the ATLAS detector using final states with two high-p T leptons. Journal of High Energy Physics, 2012, 2012, 1.	1.6	45
193	Jet mass and substructure of inclusive jets in \$ sqrt {s} = 7;{ext{TeV}} \$ pp collisions with the ATLAS experiment. Journal of High Energy Physics, 2012, 2012, 1.	1.6	88
194	Measurement of inclusive two-particle angular correlations in pp collisions with the ATLAS detector at the LHC. Journal of High Energy Physics, 2012, 2012, 1.	1.6	12
195	Hunt for new phenomena using large jet multiplicities and missing transverse momentum with ATLAS in 4.7 fbâ^'1 of \$ sqrt {s} = 7;TeV \$ proton-proton collisions. Journal of High Energy Physics, 2012, 2012, 1.	1.6	53
196	A search for \$ toverline t \$ resonances in lepton+jets events with highly boosted top quarks collected in pp collisions at \$ sqrt {s} = 7 \$ TeV with the ATLAS detector. Journal of High Energy Physics, 2012, 2012, 1.	1.6	40
197	Search for the Standard Model Higgs boson in the H → τ + Ï" â^' decay mode in \$ sqrt {s} = 7,{mathrm{ \$ pp collisions with ATLAS. Journal of High Energy Physics, 2012, 2012, 1.	TeV}} 1.6	43
198	A search for flavour changing neutral currents in top-quark decays in pp collision data collected with the ATLAS detector at \$ sqrt{s}=7;TeV \$. Journal of High Energy Physics, 2012, 2012, 1.	1.6	34

#	Article	IF	CITATIONS
199	Measurements of the pseudorapidity dependence of the total transverse energy in proton-proton collisions at \$ sqrt{s}=7 \$ TeV with ATLAS. Journal of High Energy Physics, 2012, 2012, 1.	1.6	15
200	Search for a heavy top-quark partner in final states with two leptons with the ATLAS detector at the LHC. Journal of High Energy Physics, 2012, 2012, 1.	1.6	54
201	Search for high-mass resonances decaying to dilepton final states in pp collisions at \$ sqrt{s}=7 \$ TeV with the ATLAS detector. Journal of High Energy Physics, 2012, 2012, 1.	1.6	54
202	Search for anomalous production of prompt like-sign lepton pairs at \$ sqrt{s}=7;mathrm{TeV} \$ with the ATLAS detector. Journal of High Energy Physics, 2012, 2012, 1.	1.6	17
203	Search for pair production of massive particles decaying into three quarks with the ATLAS detector in \$ sqrt{s}=7;mathrm{TeV} \$ pp collisions at the LHC. Journal of High Energy Physics, 2012, 2012, 1.	1.6	48
204	Search for R-parity-violating supersymmetry in events with four or more leptons in \$ sqrt{s}=7;mathrm{TeV} \$ pp collisions with the ATLAS detector. Journal of High Energy Physics, 2012, 2012, 1.	1.6	13
205	Tranexamic Acid Therapy in Pediatric Cardiac Surgery: A Single-Center Study. Annals of Thoracic Surgery, 2012, 94, 1302-1306.	0.7	27
206	SEU effects on power consumption in FPGAs. , 2012, , .		0
207	Electron performance measurements with the ATLAS detector using the 2010 LHC proton-proton collision data. European Physical Journal C, 2012, 72, 1.	1.4	248
208	Rapidity gap cross sections measured with the ATLAS detector in pp collisions at \$sqrt{s} = 7 mbox{~TeV}\$. European Physical Journal C, 2012, 72, 1.	1.4	100
209	Search for anomaly-mediated supersymmetry breaking with the ATLAS detector based on a disappearing-track signature in pp collisions at \$sqrt{s} = 7~mathrm{TeV}\$. European Physical Journal C, 2012, 72, 1.	1.4	13
210	Measurement of \$tar{t}\$ production with a veto on additional central jet activity in pp collisions at \$sqrt{s}=7\$ TeV using the ATLAS detector. European Physical Journal C, 2012, 72, 2043.	1.4	109
211	A search for \$tar{t}\$ resonances with the ATLAS detector in 2.05 fbâ^'1 of proton-proton collisions at \$sqrt{s} = 7~mathrm{TeV}\$. European Physical Journal C, 2012, 72, 2083.	1.4	25
212	Search for second generation scalar leptoquarks in pp collisions at \$sqrt{s}=7~mbox{TeV}\$ with the ATLAS detector. European Physical Journal C, 2012, 72, 1.	1.4	37
213	Search for a fermiophobic Higgs boson in the diphoton decay channel with the ATLAS detector. European Physical Journal C, 2012, 72, 1.	1.4	16
214	Measurement of W ± Z production in proton-proton collisions at \$sqrt{s}=7~mbox{TeV}\$ with the ATLAS detector. European Physical Journal C, 2012, 72, 1.	1.4	59
215	Search for top and bottom squarks from gluino pair production in final states with missing transverse energy and at least three b-jets with the ATLAS detector. European Physical Journal C, 2012, 72, 1.	1.4	25
216	Measurement of event shapes at large momentum transfer with the ATLAS detector in pp collisions at \$sqrt{mathbf{s}}=7 mathrm{TeV}\$. European Physical Journal C, 2012, 72, 1.	1.4	22

#	Article	IF	CITATIONS
217	Search for supersymmetry in events with large missing transverse momentum, jets, and at least one tau lepton in 7 TeV proton-proton collision data with the ATLAS detector. European Physical Journal C, 2012, 72, 1.	1.4	13
218	Search for light scalar top-quark pair production in final states with two leptons with the ATLAS detector in \$sqrt{s}=7 mathrm{TeV}\$ proton–proton collisions. European Physical Journal C, 2012, 72, 1.	1.4	31
219	ATLAS search for a heavy gauge boson decaying to a charged lepton and a neutrino in pp collisions at \$sqrt{s} = 7 mathrm{TeV}\$. European Physical Journal C, 2012, 72, 1.	1.4	36

#	Article	IF	CITATIONS
235	Measurement of inclusive jet and dijet cross sections inÂproton-proton collisions at 7ÂTeV centre-of-mass energy withÂtheÂATLAS detector. European Physical Journal C, 2011, 71, 1.	1.4	114
236	Measurement of the top quark-pair production cross section withÂATLAS in pp collisions at \$sqrt{s}=7\$ ÂTeV. European Physical Journal C, 2011, 71, 1.	1.4	146
237	Studies of the performance of the ATLAS detector using cosmic-ray muons. European Physical Journal C, 2011, 71, 1.	1.4	17
238	Luminosity determination in pp collisions at \$sqrt{s} = 7\$ TeV using the ATLAS detector at the LHC. European Physical Journal C, 2011, 71, 1.	1.4	179
239	Measurements of underlying-event properties using neutral and charged particles in pp collisions at \$sqrt{s}=900\$ GeV and \$sqrt{s}=7\$ TeV with the ATLAS detector at the LHC. European Physical Journal C, 2011, 71, 1.	1.4	31
240	Search for an excess of events with an identical flavour lepton pair and significant missing transverse momentum in \$sqrt{s}=7\$ TeV proton–proton collisions with the ATLAS detector. European Physical Journal C, 2011, 71, 1.	1.4	18
241	Search for supersymmetric particles in events with lepton pairs and large missing transverse momentum in \$sqrt{s}=7~mbox{TeV}\$ proton–proton collisions with the ATLAS experiment. European Physical Journal C, 2011, 71, 1.	1.4	41
242	Limits on the production of the standard model Higgs boson in pp collisions at \$sqrt{s} = 7\$ TeV with the ATLAS detector. European Physical Journal C, 2011, 71, 1.	1.4	40
243	Search for diphoton events with large missing transverse energy with 36 pbâ~'1 of 7 TeV proton–proton collision data with the ATLAS detector. European Physical Journal C, 2011, 71, 1.	1.4	15
244	Measurement of multi-jet cross sections in proton–proton collisions at a 7 TeV center-of-mass energy. European Physical Journal C, 2011, 71, 1.	1.4	60
245	Measurement of the jet fragmentation function and transverse profile in proton–proton collisions at a center-of-mass energy of 7 TeV with the ATLAS detector. European Physical Journal C, 2011, 71, 1.	1.4	56
246	Search for a heavy neutral particle decaying into an electron and a muon using 1 fbâ^'1 of ATLAS data. European Physical Journal C, 2011, 71, 1.	1.4	14
247	Search for massive colored scalars in four-jet final states in \$sqrt{s}=7~mbox{TeV}\$ proton–proton collisions with the ATLAS detector. European Physical Journal C, 2011, 71, 1.	1.4	39
248	Measurement of the inclusive and dijet cross-sections of b-jets in pp collisions at \$sqrt{s}=7mbox{~TeV}\$ with the ATLAS detector. European Physical Journal C, 2011, 71, 1.	1.4	73
249	Phase Noise Issues With FPGA-Embedded DLLs and PLLs in HEP Applications. IEEE Transactions on Nuclear Science, 2011, 58, 1664-1671.	1.2	7
250	Measurement of $W\hat{I}^3$ and $Z\hat{I}^3$ production in proton-proton collisions at \$ sqrt {s} = 7 \$ TeV with the ATLAS detector. Journal of High Energy Physics, 2011, 2011, 1.	1.6	11
251	Inclusive search for same-sign dilepton signatures in pp collisions at \$ sqrt {s} = 7 \$ TeV with the ATLAS detector. Journal of High Energy Physics, 2011, 2011, 1.	1.6	33
252	Search for new phenomena in final states with large jet multiplicities and missing transverse momentum using \$sqrt {s}\$ = 7 TeV pp collisions with the ATLAS detector. Journal of High Energy Physics, 2011, 2011, 1.	1.6	65

#	Article	IF	CITATIONS
253	Fixed-Latency, Multi-Gigabit Serial Links With Xilinx FPGAs. IEEE Transactions on Nuclear Science, 2011, 58, 194-201.	1.2	64
254	A FPGA-based emulation of the Timing Trigger and control receiver for the LHC experiments. , 2011, , .		1
255	The NEMO experiment data acquisition and timing distribution systems. , 2011, , .		5
256	Testing radiation tolerance of SerDeses for the SuperB experiment. , 2011, , .		3
257	Readiness of the ATLAS liquid argon calorimeter forÂLHCÂcollisions. European Physical Journal C, 2010, 70, 723-753.	1.4	61
258	The ATLAS Inner Detector commissioning and calibration. European Physical Journal C, 2010, 70, 787-821.	1.4	95
259	Drift Time Measurement in the ATLAS Liquid Argon Electromagnetic Calorimeter using Cosmic Muons. European Physical Journal C, 2010, 70, 755-785.	1.4	51
260	Commissioning of the ATLAS Muon Spectrometer withÂcosmicÂrays. European Physical Journal C, 2010, 70, 875-916.	1.4	23
261	The ATLAS Simulation Infrastructure. European Physical Journal C, 2010, 70, 823-874.	1.4	1,187
262	Readiness of the ATLAS Tile Calorimeter for LHC collisions. European Physical Journal C, 2010, 70, 1193-1236.	1.4	121
263	Performance of the ATLAS detector using first collision data. Journal of High Energy Physics, 2010, 2010, 1.	1.6	18
264	Measurement of the W → â,,"ν and Z/γ * → â,,"â,," production cross sections in proton-proton collisions at \$ s = 7;{ext{TeV}} \$ with the ATLAS detector. Journal of High Energy Physics, 2010, 2010, 1.	qrt_{s} 1.6	64
265	Development of large size Micromegas detector for the upgrade of the ATLAS Muon system. Nuclear Instruments and Methods in Physics Research, Section A: Accelerators, Spectrometers, Detectors and Associated Equipment, 2010, 617, 161-165.	0.7	51
266	Cardiac Defect with Diaphragmatic Hernia and Left Lung Agenesis – Heart Disease and Other Anomalies. Thoracic and Cardiovascular Surgeon, 2010, 58, 439-440.	0.4	5
267	Jitter issues in clock conditioning with FPGAs. , 2010, , .		5
268	Performance analysis of a DWDM optical transmission system. , 2010, , .		1
269	Characterizing Jitter Performance of Multi Gigabit FPGA-Embedded Serial Transceivers. IEEE Transactions on Nuclear Science, 2010, 57, 451-455.	1.2	22
270	Emulating the GLink Chip Set With FPGA Serial Transceivers in the ATLAS Level-1 Muon Trigger. IEEE Transactions on Nuclear Science, 2010, 57, 467-471.	1.2	7

#	Article	IF	CITATIONS
271	The Level-1 Trigger Muon Barrel System of the ATLAS experiment at CERN. Journal of Instrumentation, 2009, 4, P04010-P04010.	0.5	23
272	The ATLAS muon Micromegas R&D project: towards large-size chambers for the s-LHC. Journal of Instrumentation, 2009, 4, P12015-P12015.	0.5	10
273	High-precision time-to-digital converter in a FPGA device. , 2009, , .		8
274	The ATLAS RPC ROD for super LHC. , 2009, , .		0
275	Fast Control and Timing distribution based on FPGA-embedded serial Transceivers. , 2009, , .		1
276	Emulating the GLink chip-set with FPGA serial transceivers in the ATLAS Level-1 Muon trigger. , 2009, , .		0
277	Characterizing jitter performance of multi gigabit FPGA-embedded serial transceivers. , 2009, , .		2
278	High-Speed, Fixed-Latency Serial Links With FPGAs for Synchronous Transfers. IEEE Transactions on Nuclear Science, 2009, 56, 2864-2873.	1.2	21
279	Performance study of a DWDM link with real-time characteristics. , 2009, , .		1
280	High-precision time-to-digital converter in a FPGA device. , 2009, , .		1
281	A multi Gbit/s backplane for the RPC DAQ and L1 Trigger of the ATLAS Muon Spectrometer. Journal of Instrumentation, 2009, 4, P07015-P07015.	0.5	3
282	Beyond 320 Mbyte/s With 2eSST and Bus Invert Coding on VME64x. IEEE Transactions on Nuclear Science, 2008, 55, 203-208.	1.2	3
283	High-precision Time-to-Digital Converters in a FPGA device. , 2008, , .		1
284	High-Speed, Fixed-Latency Serial Links with FPGAs. , 2008, , .		2
285	A high speed backplane for the RPC Read Out Driver of the ATLAS Muon Spectrometer. , 2008, , .		1
286	A VLSI-FPGA system-on-Chip for detectors monitoring. , 2007, , .		0
287	FPGA implementation of a high-resolution time-to-digital converter. , 2007, , .		27
288	Beyond 320 Mbyte/s with 2eSST and Bus Invert coding on VME64x. , 2007, , .		0

0

# Article IF	
 Bus-Invert Coding for Low Noise, Low Power 2eSST VME64x Block Transfers. IEEE Transactions on Nuclear Science, 2007, 54, 616-622. 	4

290 Bus-Invert Coding For Low Noise 2eSST VME64x Block Transfers. , 2006, , .